

# Contents

<b>1</b>	<b>Theory</b>	<b>1</b>
1.1	The induced electric field equation . . . . .	1
1.2	Electric field generated by a single coil . . . . .	2
<b>2</b>	<b>Numerical discretization</b>	<b>3</b>
2.1	Finite element method . . . . .	3
2.1.1	General considerations . . . . .	3
2.1.2	Galerkin finite element equations . . . . .	3
2.1.3	Elemental matrices for triangular elements . . . . .	4
2.1.4	Boundary conditions . . . . .	6
<b>3</b>	<b>Numerical results</b>	<b>7</b>
3.1	Influence of the size of the external domain . . . . .	7
3.2	Influence of the boundary condition set on the external domain . . . . .	11
3.3	Convergence rate . . . . .	11
3.4	Influence of the electrical conductivity $\sigma$ . . . . .	11
3.5	Influence of the excitation frequency $f$ . . . . .	11
	<b>Bibliography</b>	<b>13</b>

# Chapter 1

## Theory

### 1.1 The induced electric field equation

The electromagnetic field generated by the current density flowing through the coil,  $J_{coil}$ , and that induced in the plasma,  $J_{ind}$ , is governed by the Maxwell's equations

$$\nabla \cdot \mathbf{E} = \frac{\rho}{\epsilon_0} \quad (1.1a)$$

$$\nabla \cdot \mathbf{B} = 0 \quad (1.1b)$$

$$\nabla \times \mathbf{E} = -\frac{\partial \mathbf{B}}{\partial t} \quad (1.1c)$$

$$\nabla \times \mathbf{B} = \mu_0 (\mathbf{J}_{coil} + \mathbf{J}_{ind}) + \epsilon\mu_0 \frac{\partial \mathbf{E}}{\partial t} \quad (1.1d)$$

where  $\mathbf{E}$  and  $\mathbf{B}$  are the three-dimensional components of the electric and magnetic fields,  $\mu_0$  and  $\epsilon_0$  the permeability and permittivity of the free space and  $\rho$  the charge density. The charge density  $\rho$  is supposed null because the excitation frequency is by far smaller than the fundamental frequency of the plasma, which leads to a quasi-neutral state of the plasma. Furthermore the displacement current can also be neglected, which is done by splitting the electric field  $\mathbf{E}$  into the induced electric field  $\mathbf{E}_{ind}$  and the electric field generated by the coils  $\mathbf{E}_{coils}$ . The term  $\epsilon\mu_0 \partial \mathbf{E}_{ind} / \partial t$  is removed by neglecting the electromagnetic waves and the term  $\epsilon\mu_0 \partial \mathbf{E}_{coil} / \partial t$  is removed by neglecting the electric oscillations. The Maxwell's equations boil down to

$$\nabla \cdot \mathbf{E} = 0 \quad (1.2a)$$

$$\nabla \cdot \mathbf{B} = 0 \quad (1.2b)$$

$$\nabla \times \mathbf{E} = -\frac{\partial \mathbf{B}}{\partial t} \quad (1.2c)$$

$$\nabla \times \mathbf{B} = \mu_0 (\mathbf{J}_{coil} + \mathbf{J}_{ind}) \quad (1.2d)$$

It is convenient to introduce the magnetic vector potential  $\mathbf{A}$

$$\mathbf{B} = \nabla \times \mathbf{A} \quad (1.3)$$

which, introduced in the Maxwell's equations, lead to

$$\mathbf{E} = -\frac{\partial \mathbf{A}}{\partial t} \quad (1.4a)$$

$$\nabla^2 \mathbf{A} = -\mu_0 (\mathbf{J}_{coil} + \mathbf{J}_{ind}) \quad (1.4b)$$

The induced current density is expressed by the simplified Ohm's law

$$\mathbf{J}_{ind} = \sigma \mathbf{E} = -\sigma \frac{\partial \mathbf{A}}{\partial t} \quad (1.5)$$

Further simplifications are made by assuming a sinusoidal time variation with frequency  $f$ . The classical complex notation is then used to eliminate the time variable from Eq. (1.4b). To do so let us define

$$\mathbf{J}_{coil}(\mathbf{r}, t) = \Re \left\{ \tilde{\mathbf{J}}_{coil}(\mathbf{r}) e^{i\omega t} \right\} \quad (1.6a)$$

$$\mathbf{A}(\mathbf{r}, t) = \Re \left\{ \tilde{\mathbf{A}}(\mathbf{r}) e^{i\omega t} \right\} \quad (1.6b)$$

with  $\tilde{\mathbf{J}}_{coil}$  and  $\tilde{\mathbf{A}}$  the phasors and  $\omega = 2\pi f$ . One then gets

$$\nabla^2 \tilde{\mathbf{A}} - i\mu_0 \sigma \omega \tilde{\mathbf{A}} = -\mu_0 \tilde{\mathbf{J}}_{coil} \quad (1.7)$$

Under the assumption of an axisymmetric configuration for the induction circuit, the electric current density flowing in the coil and, consequently, the magnetic vector potential will only have tangential components. The electric current density  $\tilde{\mathbf{J}}_{coil}$  is purely real so that

$$\tilde{\mathbf{J}}_{coil} = J_{coil} \bar{\mathbf{e}}_\theta \quad (1.8a)$$

$$\tilde{\mathbf{A}} = (A_\theta^r + iA_\theta^i) \bar{\mathbf{e}}_\theta \quad (1.8b)$$

$$\tilde{\mathbf{E}} = (E_\theta^r + iE_\theta^i) \bar{\mathbf{e}}_\theta = \omega (A_\theta^i - iA_\theta^r) \bar{\mathbf{e}}_\theta \quad (1.8c)$$

Equation (1.7) can then be expressed in terms of electric field and be split into the followings

$$\frac{1}{r} \frac{\partial}{\partial r} \left( r \frac{\partial E_\theta^r}{\partial r} \right) + \frac{\partial^2 E_\theta^r}{\partial z^2} - \frac{E_\theta^r}{r^2} + \mu_0 \sigma \omega E_\theta^i = 0 \quad (1.9a)$$

$$\frac{1}{r} \frac{\partial}{\partial r} \left( r \frac{\partial E_\theta^i}{\partial r} \right) + \frac{\partial^2 E_\theta^i}{\partial z^2} - \frac{E_\theta^i}{r^2} - \mu_0 \sigma \omega E_\theta^r = \mu_0 \omega J_{coil} \quad (1.9b)$$

Provided that  $J_{coil}$  is known, equations (1.9a)-(1.9b) can be solved to calculate the induced electric field. The magnetic field can then be retrieved through Eq. (1.2c)

$$B_z = B_{zr} + iB_{zi} = \frac{1}{i\omega} \frac{\partial(E_\theta^r + iE_\theta^i)}{\partial z} = \frac{1}{\omega} \frac{\partial(E_\theta^i - iE_\theta^r)}{\partial z} \quad (1.10a)$$

$$B_r = B_{rr} + iB_{ri} = -\frac{1}{i\omega} \frac{1}{r} \frac{\partial r(E_\theta^r + iE_\theta^i)}{\partial r} = \frac{1}{\omega} \frac{1}{r} \frac{\partial r(-E_\theta^i + iE_\theta^r)}{\partial r} \quad (1.10b)$$

If an electric current  $I_{coil} = J_{coil} \Omega_{coil}$  flows through the coils of section  $\Omega_{coil}$ , then one can explicit the right-hand side of Eq. (1.9b). The outer inductor is approximated by a series of  $n_r$  parallel rings of radius  $R_i$  and axial position  $Z_i$

$$J_{coil}(z, r) = \sigma E_{coil}(z, r) = -i\omega \sigma A_{coil}(z, r) = -i\omega \sigma \frac{\mu_0 I_c}{2\pi} \sum_{i=1}^{n_r} \sqrt{\frac{R_i}{r}} G(m) \quad (1.11a)$$

$$G(m) = \frac{(2-m)K(m) - 2E(m)}{\sqrt{m}} \quad (1.11b)$$

$$m = \frac{4rR_i}{(r+R_i)^2 + (Z_i - z)^2} \quad (1.11c)$$

with  $K(m)$  and  $E(m)$  being the elliptic integrals of first and second kind, respectively. The reader can find the building of the previous relations in Section 1.2.

## 1.2 Electric field generated by a single coil

## Chapter 2

# Numerical discretization

### 2.1 Finite element method

#### 2.1.1 General considerations

The finite element (FE) method introduces the concept representation of the solution by functions. The spatial domain is discretized into elements of chosen shapes (triangles, quadrangles, etc.) and equations (1.9a) and (1.9b) are solved at the corners of these elements. The solution can be interpolated inside the elements through shape functions  $N_j(r, z)$ , for which the order will fix the precision of the result. The solution at any point in the two-dimensional space is then based on the knowledge of the solution  $E_j$  at the corners of the elements:

$$E(z, r) = \sum_k N_k(z, r) E_k \quad (2.1)$$

The numerical discretization of the physical equations does not allow the strict respect of the left-hand side being equal to the right-hand side. A residual is introduced in the physical equations. The FE method is based on the weighted minimalisation of the residual over the whole domain. In order to defined the discretized equation at node  $j$ , the Galerkin FE method picks the shape function at that node  $N_j(z, r)$  as the weight factor:

$$2\pi \int_{\Omega} r N_j(z, r) \left( \nabla^2 \tilde{E}_j - i\mu_0 \sigma \omega \tilde{E}_j - i\mu_0 \omega \tilde{J}_{coilj} \right) dr dz = 0 \quad (2.2)$$

The shape functions are null everywhere except at the node  $j$  of interest. The choice of the Galerkin method has the consequence that only the direct neighbour nodes  $k$  are involved in the discretized equations at node  $j$ . These shape functions are moreover of order one because no special physical behaviour is expected.

#### 2.1.2 Galerkin finite element equations

Assuming an implicit summation over the index  $k$ , one can write down the Galerkin FE discretization of equations (1.9a) and (1.9b) at node  $j$  as

$$\int_{\Omega} r N_j \left( \frac{1}{r} \frac{\partial}{\partial r} \left( r \frac{\partial N_k}{\partial r} \right) E_{\theta k}^r + \frac{\partial^2 N_k}{\partial z^2} E_{\theta k}^r - \frac{N_k E_{\theta k}^r}{r^2} + \mu_0 \sigma \omega N_k E_{\theta k}^i \right) dr dz = 0 \quad (2.3a)$$

$$\int_{\Omega} r N_j \left( \frac{1}{r} \frac{\partial}{\partial r} \left( r \frac{\partial N_k}{\partial r} \right) E_{\theta k}^i + \frac{\partial^2 N_k}{\partial z^2} E_{\theta k}^i - \frac{N_k E_{\theta k}^i}{r^2} - \mu_0 \sigma \omega N_k E_{\theta k}^r - \mu_0 \omega J_{coil} \right) dr dz = 0 \quad (2.3b)$$

Integrating by part the two first terms of each equation allows the usage of shape functions of first order:

$$\begin{aligned} \int_{\Omega} \left( -r \frac{\partial N_j}{\partial r} \frac{\partial N_k}{\partial r} E_{\theta k}^r - r \frac{\partial N_j}{\partial z} \frac{\partial N_k}{\partial z} E_{\theta k}^r - \frac{N_j N_k E_{\theta k}^r}{r} + \mu_0 \sigma \omega r N_j N_k E_{\theta k}^i \right) dr dz \\ + \underbrace{\int_{\partial\Omega} \left( r N_j n_r \frac{\partial N_k}{\partial r} E_{\theta k}^r + r N_j n_z \frac{\partial N_k}{\partial z} E_{\theta k}^r \right) d\Gamma}_{=\int_{\partial\Omega} r N_j \frac{\partial E_{\theta}^r}{\partial n} d\Gamma=0 \text{ far field condition}} = 0 \quad (2.4a) \end{aligned}$$

$$\begin{aligned} \int_{\Omega} \left( -r \frac{\partial N_j}{\partial r} \frac{\partial N_k}{\partial r} E_{\theta k}^i - r \frac{\partial N_j}{\partial z} \frac{\partial N_k}{\partial z} E_{\theta k}^i - \frac{N_j N_k E_{\theta k}^i}{r} - \mu_0 \sigma \omega r N_j N_k E_{\theta k}^r - \mu_0 \omega r N_j J_{coil} \right) dr dz \\ + \underbrace{\int_{\partial\Omega} \left( r N_j n_r \frac{\partial N_k}{\partial r} E_{\theta k}^i + r N_j n_z \frac{\partial N_k}{\partial z} E_{\theta k}^i \right) d\Gamma}_{=\int_{\partial\Omega} r N_j \frac{\partial E_{\theta}^i}{\partial n} d\Gamma=0 \text{ far field condition}} = 0 \quad (2.4b) \end{aligned}$$

For the sake of clarity, let us define the following elemental matrices

$$m_{jk} = \int_{\Omega} r N_j N_k dr dz \quad (2.5a)$$

$$k_{jk} = - \int_{\Omega} r \left( \frac{\partial N_j}{\partial r} \frac{\partial N_k}{\partial r} + \frac{\partial N_j}{\partial z} \frac{\partial N_k}{\partial z} \right) dr dz \quad (2.5b)$$

$$p_{jk} = - \int_{\Omega} \frac{N_j N_k}{r} dr dz \quad (2.5c)$$

These matrices are dependent on the shape functions only and can be evaluated through analytical expressions for some of them, or through numerical quadratures for others. Let us also use the same paradigm for the forcing term  $J_{coil}$  as for the unknown induced electric field:  $J_{coil}(z, r) = \sum_k N_k(z, r) J_{coil,k}$ . This allows the Galerkin FE to boil down to

$$(k_{jk} + p_{jk}) E_{\theta k}^r + \mu_0 \sigma \omega m_{jk} E_{\theta k}^i = 0 \quad (2.6a)$$

$$(k_{jk} + p_{jk}) E_{\theta k}^i - \mu_0 \sigma \omega m_{jk} E_{\theta k}^r = \mu_0 \omega m_{jk} J_{coil,k} \quad (2.6b)$$

or in terms of matrix representation

$$\begin{pmatrix} k_{jk} + p_{jk} & \mu_0 \sigma \omega m_{jk} \\ -\mu_0 \sigma \omega m_{jk} & k_{jk} + p_{jk} \end{pmatrix} \begin{pmatrix} E_{\theta k}^r \\ E_{\theta k}^i \end{pmatrix} = \begin{pmatrix} 0 \\ \mu_0 \omega m_{jk} J_{coil,k} \end{pmatrix} \quad (2.7)$$

The real and imaginary components are coupled through the term  $m_{jk}$ . In the case where the electrical conductivity  $\sigma$  of the medium is null, then only the imaginary component of the induced electric field is non-zero.

### 2.1.3 Elemental matrices for triangular elements

The analytical evaluation of the elemental matrices  $m_{jk}$  and  $k_{jk}$  is more easily performed in a new  $(\eta, \xi)$  plane defined in Fig. 2.1.1. Doing so the linear shape functions take the form

$$N_1(\eta, \xi) = 1 - \eta - \xi \quad (2.8a)$$

$$N_2(\eta, \xi) = \eta \quad (2.8b)$$

$$N_3(\eta, \xi) = \xi \quad (2.8c)$$

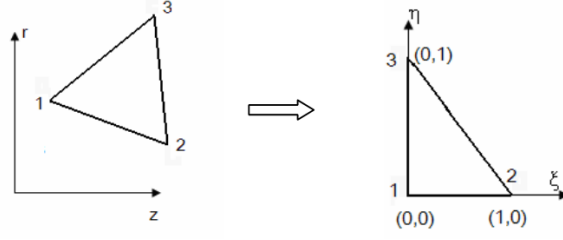


**Figure 2.1.1:** Definition of the triangular FE and its transformation to the  $(\xi, \eta)$  plane.

n	$\xi$	$\eta$	$w$	$N_1$	$N_2$	$N_3$	r
1	1/3	1/3	-27/96	1/3	1/3	1/3	$(r_1 + r_2 + r_3)/3$
2	0.2	0.6	25/96	0.2	0.2	0.6	$0.2(r_1 + r_2) + 0.6r_3$
3	0.6	0.2	25/96	0.2	0.6	0.2	$0.2(r_1 + r_3) + 0.6r_2$
4	0.2	0.2	25/96	0.6	0.2	0.2	$0.2(r_2 + r_3) + 0.6r_1$

**Table 2.1:** Quadrature table for the element matrix  $p_{jk}$ .

The integrals on this right triangle in  $(\xi, \eta)$  plane are related to the integrals on the true element (of area  $\Omega$ ) in the  $(z, r)$  plane by the Jacobian of the transformation which apply the element on the right triangle

$$\int_{\Omega} \psi(z, r) dr dz = \int_0^1 \int_0^{1-\xi} \psi(\eta, \xi) |J(\xi, \eta)| d\eta d\xi \quad (2.9)$$

where  $|J(\xi, \eta)|$  is the determinant of the Jacobian defined as

$$J(\eta, \xi) = \begin{pmatrix} \frac{\partial r}{\partial \xi} & \frac{\partial r}{\partial \eta} \\ \frac{\partial z}{\partial \xi} & \frac{\partial z}{\partial \eta} \end{pmatrix} \quad (2.10)$$

By choosing  $\psi = 1$  one gets the relation  $|J(\xi, \eta)| = 2\Omega$  which is easily computed. Let us define the normals of the segment on the other side of a node:

$$\mathbf{n}_1 = (r_3 - r_2)\bar{\mathbf{e}}_z + (z_2 - z_3)\bar{\mathbf{e}}_r \quad (2.11a)$$

$$\mathbf{n}_2 = (r_1 - r_3)\bar{\mathbf{e}}_z + (z_3 - z_1)\bar{\mathbf{e}}_r \quad (2.11b)$$

$$\mathbf{n}_3 = (r_2 - r_1)\bar{\mathbf{e}}_z + (z_1 - z_2)\bar{\mathbf{e}}_r \quad (2.11c)$$

Then the analytical expressions for the elemental matrices  $m_{jk}$  and  $k_{jk}$  are (see Detandt [1])

$$m_{jk} = \frac{\Omega(r_1 + r_2 + r_3 + r_j + r_k)(1 + \delta_{jk})}{60} \quad (2.12a)$$

$$k_{jk} = -\frac{(r_1 + r_2 + r_3)(n_j^r n_k^r + n_j^z n_k^z)}{12\Omega} \quad (2.12b)$$

The elemental matrix  $p_{jk}$  requires a numerical quadrature because of the difficulty to evaluate analytically. For this purpose, four internal quadrature points are taken in order to avoid any singularity at  $r = 0$  (see Table 2.1):

$$p_{jk} = -\int_{\Omega} \frac{N_j N_k}{r} dr dz = -\sum_{n=1}^4 w_n \frac{N_j(\eta_n, \xi_n) N_k(\eta_n, \xi_n)}{r_n} |J(\xi, \eta)| \quad (2.13)$$

#### 2.1.4 Boundary conditions

The induced electric field must satisfy boundary conditions so that the system of equations built by the numerical method can be solved. On the axis, the vanishing condition is imposed

$$E(z, 0) = 0 \quad (2.14)$$

whereas two different far field boundary conditions are considered for the outer domain

$$E(z, r) = 0, \quad (2.15a)$$

$$\text{or} \quad \frac{\partial E}{\partial n} = 0 \quad (2.15b)$$

The first one will overwrite the equations at the nodes on the outer boundary, whereas the second one cancels the boundary integral from Eqs. (2.4). In the later case, the equations are solved at the nodes on the outer boundary.

## Chapter 3

# Numerical results

This chapter displays the results of the resolution of Equations (2.7) inside and around an inductively coupled plasma torch. The geometry of the whole domain and detail of the VKI minitorch are shown in Fig. 3.0.1. This minitorch has a diameter of  $3cm$ , an excitation frequency of  $27MHz$  and works with argon. The following sections will study

- the influence of the radius  $R$  of the external domain,
- the influence of the type of boundary condition set at the far field,
- the convergence rate of the numerical method as a function of degrees of freedom inside the torch,
- the influence of the electrical conductivity  $\sigma$  on the solution,
- the influence of the excitation frequency  $f$  of the coils

### 3.1 Influence of the size of the external domain

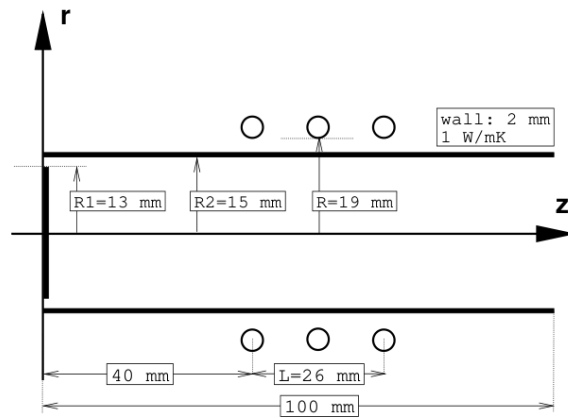
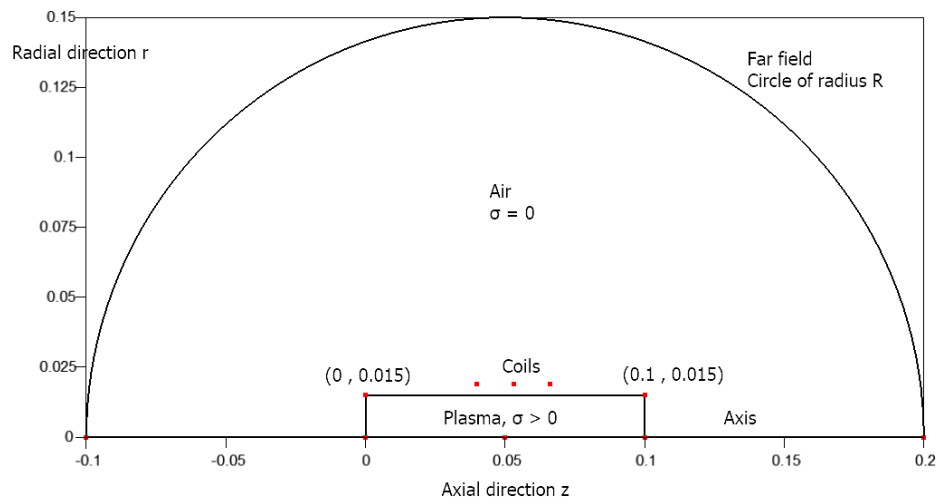
The external domain surrounding the torch is a circle centered on the torch, of radius  $R$  (see Fig. 3.0.1). The radius  $R$  of the circle is increased from  $0.1m$  to  $1.0m$  by increment of  $0.1m$  and the two types of boundary conditions on the outer boundary (Section 2.1.4) are tested here. Three values of the electrical conductivity are taken ( $\sigma = 10^2, 10^3$  and  $10^4 S/m$ ) and the excitation frequency is set to  $27MHz$ .

The largest radius is chosen as reference and the relative error for both real and imaginary parts of the electric field is defined as

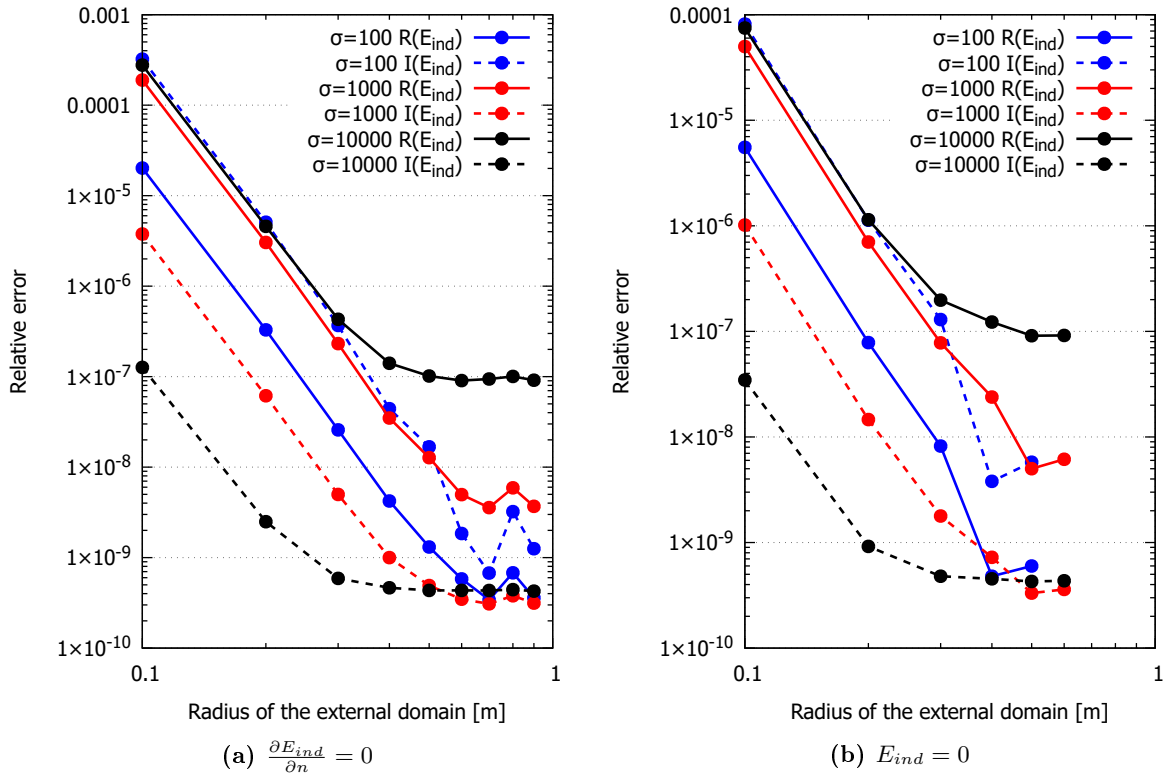
$$\epsilon_{rel} = \sqrt{\frac{\sum_m (E_m - E_m^{R=1})^2}{\sum_m (E_m^{R=1})^2}} \quad (3.1)$$

Figure 3.1.1 shows the relative error for both boundary conditions at the outer edge, as a function of the radius  $R$ . For both boundary conditions type, the solution seems to be radius-independent for  $R = 0.6m$ .





**Figure 3.0.1:** Geometry of the VKI minitorch (vanden Abeele [2]).



**Figure 3.1.1:** Influence of the size of the external domain on the solution. Cut at  $z = 0.053m$  located at the middle coil.

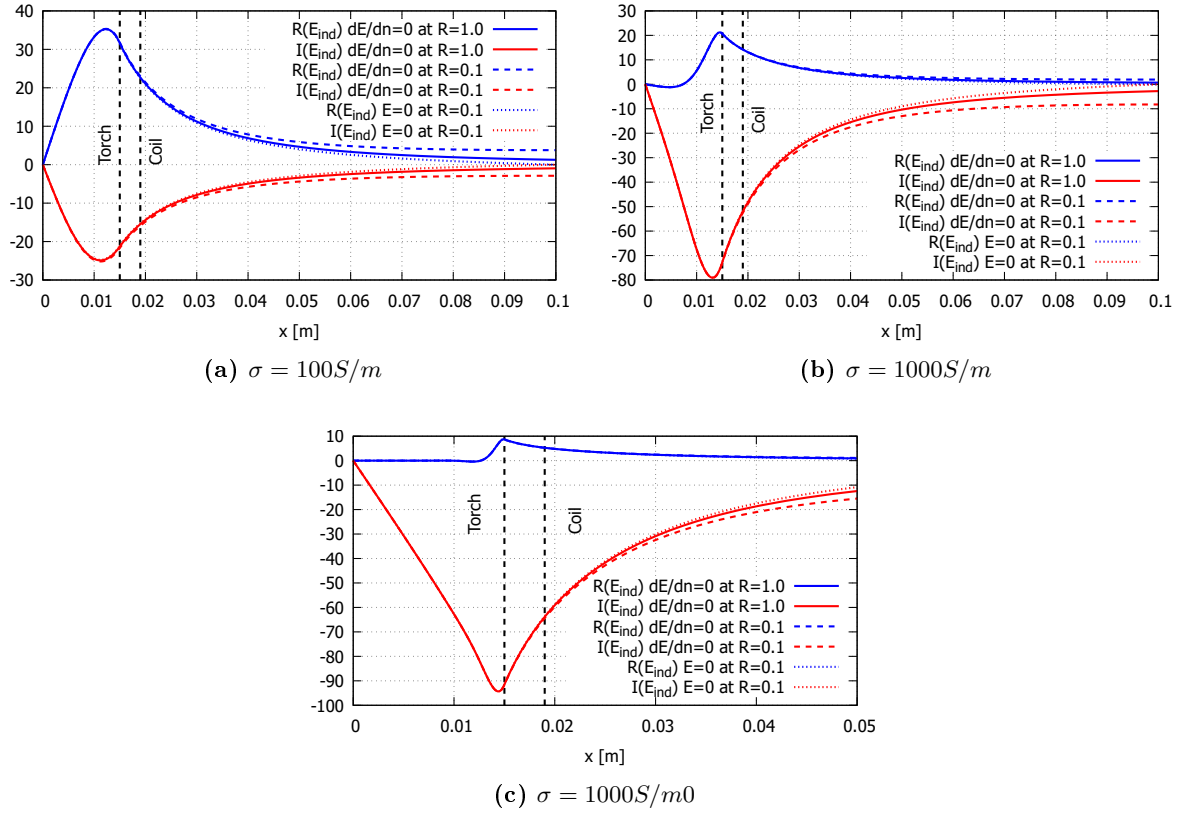


**Figure 3.2.1:** Influence of the boundary condition set on the external domain. Cut at  $z = 0.053m$  located at the middle coil.

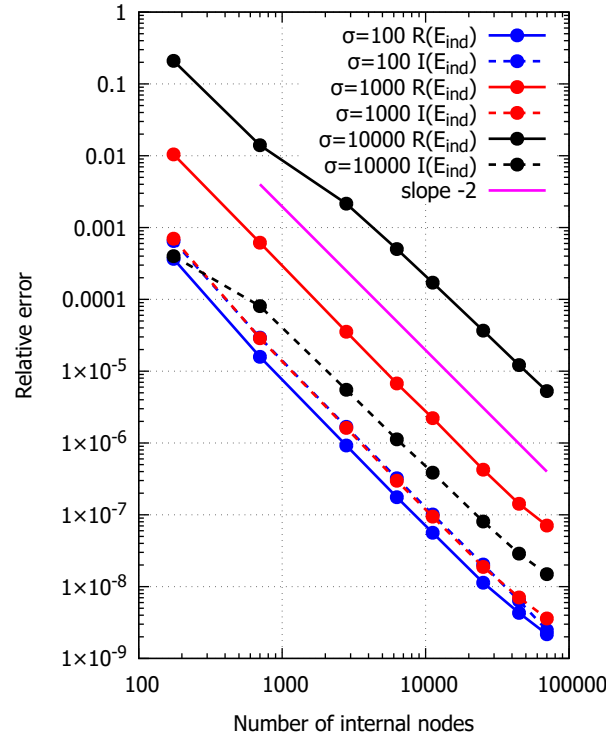


**Figure 3.3.1:** Convergence rate

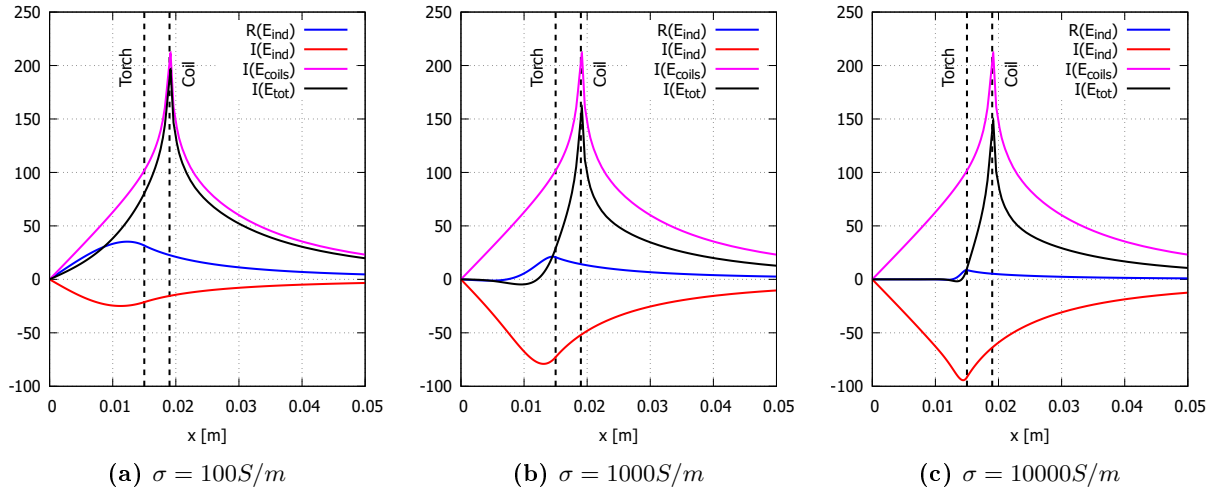


**Figure 3.4.1:** Influence of the electrical conductivity  $\sigma$  on the solution. Cut at  $z = 0.053m$  located at the middle coil.

### 3.2 Influence of the boundary condition set on the external domain

### 3.3 Convergence rate

### 3.4 Influence of the electrical conductivity $\sigma$

### 3.5 Influence of the excitation frequency $f$

Ecoil directly proportional to  $f$

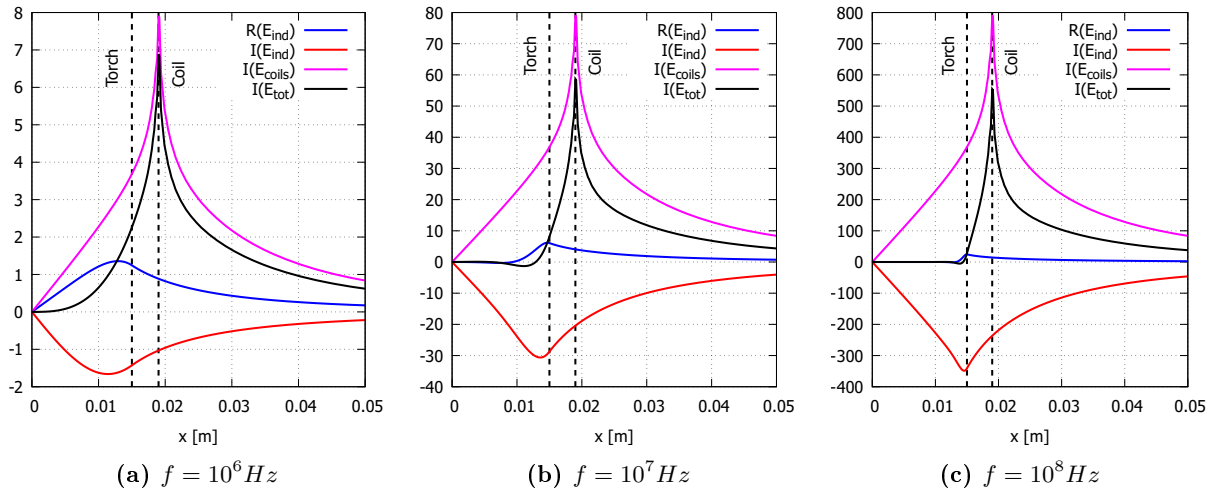


**Figure 3.5.1:** Influence of the excitation frequency  $f$  on the solution. Cut at  $z = 0.053m$  located at the middle coil.

# Bibliography

- [1] Yves Detandt. *Extension of Spectral/Finite Element solver for Large Eddy Simulation (SFE-LES) for axisymmetric bodies*. PhD thesis, Université Libres de Bruxelles, 2004.
- [2] David vanden Abeele. *An efficient computational model for inductively coupled air plasma flows under thermal and chemical non-equilibrium - with application to atmospheric re-entry flow studies*. PhD thesis, Katholieke Universiteit Leuven, 2000.